Data documentation: Example

(From Pfänder et al., 2018, J. Petrol., 59, 667-694)

Table 1: Major element, trace element and isotope data of SiO_2-undersaturated rocks from the Heldburg region

Sample Rock type	Method	S097511 Mel	S097512 Mel	S097519 Mel	S107048 Mel	S107052 Mel	S097513 Neph	S097514 Neph	S097515 Neph	S107045 Neph
SiO_2	XRF	35·5	34·9	35·4	34·5	34·2	38·4	41·0	41·3	40·0
Al_2O_3	XRF	9·00	9·42	9·09	9·60	9·52	9·6	11·1	11·1	10·3
Fe_2O_3	XRF	12·9	12·2	11·8	13·4	11·6	12·0	12·6	13·1	13·3
FeO		11·6	10·9	10·6	12·0	10·4	10·8	11·4	11·8	11·9
MnO	XRF	0·20	0·18	0·17	0·18	0·17	0·17	0·20	0·20	0·20
MgO	XRF	13·3	12·8	14·0	13·3	14·1	13·6	12·3	12·6	13·7
CaO	XRF	12·0	11·6	12·5	11·6	12·7	11·2	11·8	11·3	11·9
Na_2O	XRF	3·39	3·16	3·47	3·11	3·82	2·92	4·04	3·44	3·26
K_2O	XRF	1·35	1·25	0·98	1·16	0·74	0·79	1·08	1·14	0·95
TiO_2	XRF	2·85	2·84	2·67	2·90	2·53	2·80	2·84	2·94	2·89
P_2O_5	XRF	1·00	0·99	0·84	0·76	0·82	0·61	0·82	0·77	0·86
SO_3	XRF	1·11	0·84	0·71	0·28	0·46	0·31	0·03	0·05	0·06
L·O·I	XRF	7·60	9·86	8·94	9·48	9·92	8·42	2·04	2·12	2·96
SUM	XRF	100·3	99·9	100·5	100·3	100·6	100·8	99·9	100·1	100·3
Li	ICPMS	36·9	31·6	45·2	15·5	54·6	20·0	41·5	21·1	27·2
Sc	ICPMS	20·7	20·1	22·3	21·9	26·2	21·3	21·9	24·8	24·3
V	XRF	265	265	228	272	246	262	279	281	289
Cr	XRF	494	458	409	367	539	451	476	527	643
Co	ICPMS	72·8	53·5	66·5	70·0	61·0	74·4	64·9	69·0	74·6
Ni	XRF	424	206	354	309	379	385	312	325	468
Cu	XRF	188	254	133	146	144	185	113	158	178
Zn	XRF	173	193	117	137	104	163	129	163	185
Ga	ICPMS	16·4	17·8	15·9	18·0	16·2	16·6	17·8	18·0	17·1
Rb	ICPMS	33·1	42·4	25·0	30·8	22·1	14·7	18·0	32·1	16·3
Sr	XRF	1361	1104	959	815	988	807	1105	1083	982
Y	ICPMS	29·0	30·0	23·5	23·4	23·5	21·1	27·3	26·9	25·2
Zr	XRF	321	307	266	299	225	230	264	264	286
Nb	ICPMS	106·3	117·6	91·1	96·5	99·9	72·5	97·5	91·7	92·3
Cs	ICPMS	0·677	0·485	0·392	0·302	0·299	2·50	1·32	1·06	0·976
Ba	XRF	828	778	797	2961	719	657	870	828	788
La	ICPMS	109·2	109·3	80·5	75·3	77·2	62·4	96·0	89·1	81·6
Ce	ICPMS	208	208	146	147	141	125	182	168	154
Pr	ICPMS	23·8	23·9	16·8	16·8	15·3	15·1	20·6	19·2	17·7
Nd	ICPMS	88·5	88·3	65·5	63·9	55·6	59·1	76·6	73·0	67·0
Sm	ICPMS	14·3	14·5	11·1	11·2	10·4	9·8	12·5	12·1	11·2
Eu	ICPMS	4·47	4·55	3·54	3·53	3·24	3·25	3·97	3·88	3·53
Gd	ICPMS	11·88	12·18	9·48	9·31	8·44	8·90	10·58	10·36	9·45
Tb	ICPMS	1·55	1·60	1·23	1·23	1·08	1·18	1·42	1·36	1·20

(continued)

Table 1: Continued

Sample Rock type	Method	S097511 Mel	S097512 Mel	S097519 Mel	S107048 Mel	S107052 Mel	S097513 Neph	S097514 Neph	S097515 Neph	S107045 Neph
Dy	ICPMS	8·09	8·50	6·45	6·35	5·81	6·15	7·51	7·24	6·48
Ho	ICPMS	1·32	1·40	1·09	1·02	0·969	1·02	1·25	1·24	1·08
Er	ICPMS	3·09	3·31	2·54	2·48	2·35	2·36	3·11	2·98	2·63
Tm	ICPMS	0·362	0·406	0·301	0·274	0·279	0·286	0·379	0·358	0·331
Yb	ICPMS	1·73	1·89	1·48	1·40	1·54	1·32	1·84	1·78	1·67
Lu	ICPMS	0·238	0·262	0·199	0·188	0·214	0·180	0·252	0·245	0·238
Hf	ICPMS	7·11	7·17	6·18	7·03	5·46	5·62	6·10	6·06	6·44
Ta	ICPMS	5·57	5·92	4·72	5·31	4·83	4·11	4·92	4·79	5·05
Pb	ICPMS	13·36	11·99	8·72	6·73	4·89	8·20	7·75	7·93	8·77
Th	ICPMS	14·02	14·00	10·30	8·26	9·34	7·74	12·40	11·07	9·40
U	ICPMS	4·01	3·27	3·29	2·16	1·41	2·36	3·69	3·33	2·93
$(^{206}Pb/^{204}Pb)_m$		18·72	18·54	18·87	18·57	18·92	18·56	18·95	18·67	18·49
$(^{206}Pb/^{204}Pb)i$		18·61	18·45	18·73	18·47	18·82	18·47	18·77	18·55	18·41
$(^{207}Pb/^{204}Pb)_m$		15·62	15·60	15·61	15·61	15·61	15·62	15·64	15·61	15·62
$(^{207}Pb/^{204}Pb)i$		15·61	15·60	15·60	15·61	15·61	15·62	15·63	15·60	15·62
$(^{208}Pb/^{204}Pb)_m$		38·65	38·42	38·77	38·49	38·78	38·49	38·88	38·57	38·42
$(^{208}Pb/^{204}Pb)i$		38·52	38·29	38·62	38·36	38·57	38·40	38·68	38·44	38·33
$(^{176}Hf/^{177}Hf)_m$		0·282881±4	0·282879±4	0·282894±5	0·282868±5	0·282922±4	–	0·282858±7	0·282867±6	0·282917±6
$(^{176}Hf/^{177}Hf)i$		0·282878	0·282876	0·282891	0·282865	0·282919		0·282854	0·282864	0·282914
$e_{Hf(0)}$		3·9	3·8	4·3	3·4	5·3	–	3·0	3·4	5·1
$e_{Hf(i)}$		3·7	3·7	4·2	3·3	5·2		2·9	3·3	5·0
$(^{143}Nd/^{144}Nd)_m$		0·512858±7	0·512846±7	0·512866±10	0·512856±10	0·512879±8	–	0·512838±9	0·512844±8	0·512881±8
$(^{143}Nd/^{144}Nd)i$		0·512839	0·512825	0·512841	0·512834	0·512855	–	0·512813	0·512824	0·512864
$e_{Nd(0)}$		4·3	4·1	4·5	4·2	4·7	–	3·9	4·0	4·7
$e_{Nd(i)}$		4·7	4·5	4·9	4·6	5·1		4·4	4·4	5·0
$(^{87}Sr/^{86}Sr)_m$		0·705187±12	0·704482±11	0·703682±13	0·703687±13	0·703970±32	–	0·703686±11	0·703740±11	0·703517±21
$(^{87}Sr/^{86}Sr)_i$		0·70515	0·70443	0·70364	0·703637	0·703939		0·70366	0·70370	0·70350

(continued)

Data documentation: Example

(From Romer et al., 2010, N. Jb. Miner. Abh., 187, 289-305)

Table 2. U–Pb analytical data of zircon from the microgranite dike at Písečný vrch, Teplice region, Czech Republic.

Sample[a]	Weight (mg)	Concentrations (ppm)		$^{206}Pb/^{204}Pb$	$^{232}Th/^{238}U$	Radiogenic Pb (at%)[c]				Atomic ratios[c]			Apparent ages (Ma)[d]		
		U	Pb_{tot}	Measured ratios[b]	(at)[c]	^{206}Pb	^{207}Pb	^{208}Pb	$^{238}U/^{204}Pb$	$^{206}Pb/^{238}U$	$^{207}Pb/^{235}U$	$^{207}Pb/^{206}Pb$	$^{206}Pb/^{238}U$	$^{207}Pb/^{235}U$	$^{207}Pb/^{206}Pb$
Abraded zircon															
1	0.067	220.6	11.90	988	0.51	82.48	4.35	13.16	29100	0.04964	0.3613	0.05279	312	313	320
2	0.103	203.2	11.65	646	0.55	81.64	4.31	14.05	14600	0.05034	0.3665	0.05281	317	317	321
3	0.033	188.0	9.97	1010	0.53	81.94	4.32	13.74	77800	0.04977	0.3614	0.05266	313	313	314
4	0.038	197.3	12.58	350	0.59	80.87	4.29	14.84	8020	0.05253	0.3845	0.05309	330	330	333
5	0.052	211.1	13.04	549	0.52	82.14	4.39	13.47	12640	0.05419	0.3997	0.05339	340	341	350
6	0.087	221.4	14.44	694	0.54	81.59	4.48	13.92	13400	0.05754	0.4360	0.05496	360	367	411
7	0.110	184.1	10.75	727	0.59	80.70	4.25	15.04	16600	0.05119	0.3720	0.05270	322	321	316
8	0.088	92.7	5.32	750	0.56	81.36	4.30	14.34	24000	0.05154	0.3752	0.05279	324	324	320
9	0.087	215.4	14.88	200	0.56	81.46	4.25	14.29	3840	0.04986	0.3587	0.05217	314	311	293
10	0.024	506.4	30.27	723	0.62	80.16	4.25	15.59	18400	0.05249	0.3837	0.05301	330	330	329
11	0.095	216.7	12.47	326	0.56	81.46	4.30	14.24	7200	0.04623	0.3365	0.05280	292	295	320
12	0.096	269	18.86	405	0.52	82.10	4.55	13.35	7100	0.05833	0.4455	0.05539	366	374	428
13	0.132	169	19.36	69.6	0.58	80.99	4.53	14.66	1030	0.05041	0.3735	0.05374	317	322	360
Weakly abraded and broken zircon															
14	0.133	125.6	18.46	52.3	0.59	80.71	4.26	15.04	680	0.05082	0.3697	0.02753	320	319	318
15	0.128	131.3	41.4	29.95	0.68	79.18	4.03	16.79	240	0.0494	0.347	0.0509	311	302	236
16	0.121	182.2	13.35	172	0.59	80.88	4.27	14.85	3200	0.05017	0.3650	0.05277	316	316	319
Non-abraded zircon															
17															
18	0.146	277.3	17.25	184	0.70	77.99	4.95	17.06	4030	0.04221	0.3695	0.06350	267	319	725
19	0.222	953	123.9	54.0	0.58	81.09	4.22	14.69	778	0.04619	0.3315	0.05204	291	291	287
20	0.222	180.3	10.2	199	0.61	79.61	5.04	15.35	4660	0.03984	0.3476	0.06327	252	303	717
21	0.154	356.8	30.95	87.3	0.54	81.79	4.37	13.84	1570	0.04434	0.3268	0.05344	280	287	348
22	0.445	232.5	14.04	226	0.66	78.75	4.99	16.26	4860	0.04335	0.3785	0.06332	274	326	719

[a] Zircon concentrates were cleaned in warm 7N HNO_3 and H_2O before dissolution in concentrated HF in teflon-lined autoclaves at 210 °C for 4 days. A mixed ^{205}Pb-^{235}U tracer was added before sample dissolution. Lead and U were separated using ion-exchange chromatographic p rocedures (e.g., Romer et al. 1996; Schmid et al. 2003). Lead and U were loaded together on single Re-filaments using a silica-gel emitter and H_3PO_4 (Gerstenberger & Haase 1997) and measured at 1200°–1260 °C and 1350–1400 °C, respectively, on a Finnigan MAT262 multicollector mass-spectrometer (modified with an ion source by Spectromat) using Faraday collectors and ion counting.

[b] Lead isotope ratios corrected for fractionation (0.1 % / a.m.u.).

[c] Lead corrected for fractionation, blank, tracer contribution, and initial lead ($^{206}Pb/^{204}Pb = 18.1 \pm 0.1$, $^{207}Pb/^{204}Pb = 15.60 \pm 0.02$, $^{208}Pb/^{204}Pb = 38.2 \pm 0.2$). During the measurement period, total blanks were < 15 pg for lead and < 1 pg for uranium. $^{232}Th/^{238}U$ ratios calculated for an age of 320 Ma from $^{208}Pb_{rad}/^{206}Pb_{rad}$.

[d] Apparent ages were calculated using the constants recommended by IUGS (Steiger & Jäger 1977).

Calculation of melt volume and composition I

McKenzie (1984) The generation and compaction of partially molten rock, J. Petrol., 25, 713-765. McKenzie & Bickle, 1988, The volume and composition of melt generated by extension of the lithosphere, J. Petrol., 29, 625-679.

TABLE 1

Notation

Variable	*Meaning*	*Value used*	*Dimensions*
a	particle radius	10^{-3}	m
$\mathbf{a}_z$	unit vector in vertical		none
C_p	specific heat at constant pressure	10^3	$J\ kg^{-1}\ K^{-1}$
C_p^f	specific heat of melt at constant pressure		$J\ kg^{-1}\ K^{-1}$
C_p^s	specific heat of matrix at constant pressure		$J\ kg^{-1}\ K^{-1}$
c_f	concentration by weight in the melt		none
c_s	concentration by weight in the matrix		none
D_{11}	horizontal diffusivity		$m^2\ s^{-1}$
D_{33}	vertical diffusivity		$m^2\ s^{-1}$
D_b	grain boundary diffusivity		$m^2\ s^{-1}$
D_f	diffusivity of melt (Hofmann & Magaritz, 1977)	10^{-10}	$m^2\ s^{-1}$
D_s	diffusivity of matrix (Hofmann & Hart, 1978; Miyamoto & Takeda, 1983)	10^{-17}	$m^2\ s^{-1}$
g	acceleration due to gravity	9·81	$m\ s^{-2}$
H	rate of internal heat generation		$J\ m^{-3}\ s^{-1}$
h	depth of a layer		m
K_c	$= c_s/c_f$ partition coefficient between matrix and melt		none
k	Boltzmann's constant		$J\ K^{-1}$
k_T	effective thermal conductivity of melt and matrix equation (A38)		$Wm^{-1}\ K^{-1}$
k_T^f	thermal conductivity of melt		$Wm^{-1}\ K^{-1}$
k_T^s	thermal conductivity of matrix		$Wm^{-1}\ K^{-1}$
k_ϕ	specific permeability		m^2
$\mathbf{I}$	body force on the matrix from melt movement		$N\ m^{-3}$
L	latent heat of melting		$J\ kg^{-1}$
l	length scale		m
$\frac{D_v M}{Dt}$	the rate of conversion of matrix into melt/unit volume, measured in a frame fixed to the matrix		$kg\ m^{-3}\ s^{-1}$
P	pressure		Pa
P_f	pressure in melt		Pa
P_s	presure in solid		Pa
Ra	Rayleigh number for convection in a porous medium equation (3.9)		none
Re	$= \lvert\mathbf{v}\rvert\ l/\nu$ Reynolds number		none
S_f	entropy of the melt		$J\ kg^{-1}\ K^{-1}$
S_s	entropy of the solid		$J\ kg^{-1}\ K^{-1}$
ΔS	entropy change on melting	362	$J\ kg^{-1}\ K^{-1}$
T	absolute temperature		K
T_s	solidus temperature		K
ΔT	temperature difference between liquidus and solidus		K
t	time		s
t'	$= t/\tau_0$ dimensionless time		none
t_f	total melt thickness		km
$\mathbf{V}$	$= (U, V, W)$ velocity of matrix		$m\ s^{-1}$
$\mathbf{v}$	$= (u, v, w)$ velocity of melt in pores		$m\ s^{-1}$
ΔV	volume change on melting $= \left(\frac{1}{\rho_f} - \frac{1}{\rho_s}\right)$		$m^3\ kg^{-1}$

Calculation of melt volume and composition II

McKenzie (1984) The generation and compaction of partially molten rock, J. Petrol., 25, 713-765. McKenzie & Bickle, 1988, The volume and composition of melt generated by extension of the lithosphere, J. Petrol., 29, 625-679.

Variable	*Meaning*	*Value used*	*Dimensions*
W'	$= W/w_0$ dimensionless vertical matrix velocity		none
w'	$= w/w_0$ dimensionless vertical melt velocity		none
w_e	transport velocity of solute, equation (5.3)		$m\ s^{-1}$
w_0	reference vertical velocity, the minimum fluidization velocity, equation (B7)		$m\ s^{-1}$
X	melt fraction by weight		none
x, y	horizontal coordinates		m
x'	$= x/\delta_c$ dimensionless		none
y'	$= y/\delta_c$ horizontal coordinates		
z	vertical coordinate, positive upwards		m
z'	$= z/\delta_c$ dimensionless vertical coordinate		none
α_f	thermal expansion coefficient of melt (Dane, 1941)	$6{\cdot}8 \times 10^{-5}$	K^{-1}
α_s	thermal expansion coefficient of matrix	4×10^{-5}	K^{-1}
γ_{sf}	grain boundary energy between matrix and melt		$N\ m^{-1}$
γ_{ss}	grain boundary energy between matrix grains		$N\ m^{-1}$
δ	grain boundary thickness		m
δ_c	$= \left[\frac{(\zeta + \frac{4}{3}\eta)}{\mu} k_\phi\right]^{1/2}$ compaction length		m
ζ	$= (1-\phi)\,\zeta^x$ effective bulk viscosity of matrix	10^{15}	Pa s
ζ^x	bulk viscosity of matrix		Pa s
η	$= (1-\phi)\,\eta^x$ effective dynamic shear viscosity of matrix	10^{15}	Pa s
η^x	shear viscosity of matrix		Pa s
Θ	dihedral angle, Fig. 4*a*	$50°$	
κ_T	effective thermal diffusivity of melt and matrix, equation (A40)	10^{-6}	$m^2\ s^{-1}$
μ	dynamic shear viscosity of melt (Murase & McBirney, 1973)	1	Pa s
ν	$= \mu/\rho_f$ kinematic shear viscosity of melt		$m^2\ s^{-1}$
ρ_f	density of melt	$2{\cdot}8 \times 10^3$	$kg\ m^{-3}$
ρ_s	density of matrix	$3{\cdot}3 \times 10^3$	$kg\ m^{-3}$
$\bar{\rho}$	$= (1-\phi)\,\rho_s + \phi\rho_f$ mean density of melt and matrix		$kg\ m^{-3}$
$\boldsymbol{\sigma}$	$\equiv \sigma_{ij}$ stress tensor		Pa
$\boldsymbol{\sigma}'$	$\equiv \sigma'_{ij}$ deviatoric stress tensor in matrix		Pa
$\boldsymbol{\sigma}^f$	$\equiv \sigma^f_{ij}$ stress tensor in melt		Pa
$\boldsymbol{\sigma}^s$	$\equiv \sigma^s_{ij}$ stress tensor in matrix		Pa
τ	a characteristic time		s
τ_0	reference time, characteristic time for compaction equation (B11)		s
ϕ	porosity of matrix		none
ϕ_0	initial porosity of matrix		none
ϕ_I	isolated porosity		none
Ω	Atomic volume		m^3
∇'	$= \delta_c \nabla$ dimensionless vector operator		none

Average global composition of MORB

Gale et al., 2013: The mean composition of ocean ridge basalts. Geochemistry, Geophysics, Geosystems.

Table 1. The Composition of ALL MORB[a]

	n	ALL MORB Mean[b]	± (95% conf)	ALL MORB Log-Normal Mean[c]	± (95% conf)	Upper Bound	Lower Bound
MgO	430	**7.58**	0.12	7.69	0.08	9.04	6.21
SiO_2	430	**50.47**	0.08	50.41	0.08	51.75	49.22
FeO	430	**10.43**	0.21	10.07	0.14	13.48	8.12
CaO	430	**11.39**	0.09	11.35	0.07	12.49	10.15
Na_2O	430	**2.79**	0.03	2.76	0.04	3.69	2.06
Al_2O_3	430	**14.70**	0.12	14.95	0.10	16.74	13.25
TiO_2	430	**1.68**	0.05	1.54	0.03	2.32	1.06
K_2O	430	**0.160**	0.014	0.144	0.011	0.558	0.045
P_2O_5	409	**0.184**	0.012	0.169	0.008	0.400	0.082
MnO	379	**0.184**	0.005	0.173	0.004	0.231	0.105
Ba	392	**29.2**	3.8	23.1	2.7	160.3	3.9
Be	139	**0.76**	0.05	0.64	0.05	1.22	0.25
Ce	410	**14.86**	1.26	12.99	0.70	33.18	5.09
Co	350	**43.0**	0.7	42.9	0.5	53.0	35.9
Cr	369	**249**	12	251	11	406	81
Cs	272	**0.034**	0.006	0.029	0.004	0.175	0.006
Cu	357	**74**	2	75	2	122	57
Dy	411	**6.08**	0.30	5.43	0.17	8.83	3.66
Er	410	**3.79**	0.17	3.37	0.10	5.71	2.28
Eu	411	**1.36**	0.05	1.25	0.03	2.02	0.81
Ga	300	**17.5**	0.2	17.1	0.2	20.0	14.6
Gd	386	**4.99**	0.23	4.51	0.14	7.56	2.98
Hf	398	**2.79**	0.15	2.44	0.10	4.51	1.26
Ho	404	**1.28**	0.05	1.16	0.03	1.85	0.78
La	412	**5.21**	0.53	4.51	0.30	16.32	1.43
Li	255	**6.5**	0.3	6.0	0.2	9.1	3.7
Lu	410	**0.53**	0.02	0.48	0.01	0.83	0.32
Mo	185	**0.46**	0.05	0.41	0.04	1.24	0.16
Nb	402	**5.24**	0.59	4.11	0.38	24.50	1.01
Nd	418	**12.03**	0.78	10.81	0.45	22.55	5.40
Ni	365	**92**	5	97	4	183	44
Pb	370	**0.57**	0.03	0.53	0.03	1.31	0.20
Pr	390	**2.24**	0.12	2.05	0.09	4.15	0.92
Rb	380	**2.88**	0.44	2.15	0.27	13.87	0.37
Sc	338	**39.8**	0.8	38.8	0.6	49.2	29.5
Sm	417	**3.82**	0.15	3.49	0.10	6.17	2.06
Sn	200	**0.92**	0.06	0.79	0.05	1.63	0.28
Sr	413	**129**	4	129	5	246	70
Ta	352	**0.34**	0.04	0.27	0.03	1.44	0.07
Tb	397	**0.90**	0.04	0.82	0.02	1.31	0.53
Th	395	**0.404**	0.081	0.292	0.033	2.135	0.059
Tl	200	**0.020**	0.001	0.019	0.001	0.041	0.006
U	374	**0.119**	0.013	0.095	0.009	0.495	0.022
V	337	**309**	13	287	7	396	194
W	209	**0.12**	0.02	0.10	0.01	0.40	0.01
Y	410	**36.8**	1.9	32.6	1.0	53.6	21.5
Yb	411	**3.63**	0.18	3.23	0.10	5.80	2.15
Zn	338	**91.3**	3.1	86.6	1.9	119.5	59.9
Zr	412	**116.9**	8.4	100.7	4.4	220.0	49.9
$^{87}Sr/^{86}Sr$	272	**0.702819**	0.000067				
$^{143}Nd/^{144}Nd$	272	**0.513074**	0.000017				
$^{206}Pb/^{204}Pb$	245	**18.412**	0.090				
$^{207}Pb/^{204}Pb$	245	**15.515**	0.010				
$^{208}Pb/^{204}Pb$	245	**38.100**	0.091				
$^{176}Hf/^{177}Hf$	138	**0.283**	0.000				
Sm/Nd	416	**0.325**	0.005				
Zr/Hf	398	**40.64**	0.95				
Ba/Th	376	**71.93**	8.32				
Nb/U	366	**44.37**	1.99				

Experimentally determined composition of melts in equilibrium with spinel peridotite KLB-1 at various pressures and temperatures (Hirose & Kushiro, 1993, Partial melting of dry peridotites at high pressures: Determination of compositions..., Earth Planet. Sci. Lett., 114, 477-489)

KLB-1

Run	14	15	16	17	18	19	20
P (kbar)	10	10	10	10	15	15	15
T (°C)	1250	1300	1350	1400	1300	1350	1400
SiO_2	51.32	50.49	50.67	51.59	50.71	49.13	49.88
TiO_2	1.09	0.65	0.42	0.44	1.04	0.60	0.45
Al_2O_3	19.09	17.94	14.61	12.58	19.31	15.18	13.78
FeO*	6.38	6.69	7.64	7.95	6.37	7.54	7.92
MnO	0.23	0.11	0.13	0.29	0.14	0.14	0.13
MgO	8.14	10.08	13.39	16.41	8.31	13.11	15.74
CaO	8.85	11.37	11.17	9.42	7.75	12.28	10.69
Na_2O	4.60	2.47	1.50	0.91	5.47	1.58	1.04
K_2O	0.27	0.09	0.19	0.05	0.73	0.08	0.04
Cr_2O_3	0.03	0.11	0.28	0.36	0.17	0.36	0.33
Total	100.00	100.00	100.00	100.00	100.00	100.00	100.00
CIPW norm							
os	1.54	0.36	1.13	0.30	4.33	0.47	0.24
ab	33.78	19.68	12.72	7.70	29.61	13.45	8.80
an	30.69	38.45	32.66	30.21	26.04	34.19	32.93
ne	2.79				9.07		
di	10.70	14.63	18.43	13.37	10.06	21.67	16.25
hy		15.41	24.12	43.84		12.45	28.92
ol	18.42	10.23	10.13	3.75	18.93	16.63	12.01
il	2.08	1.24	0.80	0.84	1.96	1.14	0.85
Fo (mol%)	89.2	89.9	91.0	93.1	89.5	90.6	91.5
K_d (Fe/Mg)	0.275	0.302	0.309	0.273	0.273	0.321	0.329
F [a]	0.065	0.121	0.200	0.331	0.055	0.189	0.289

KLB-1

Run	21	22	23	24	25	26
P (kbar)	20	20	25	25	30	30
T (°C)	1375	1425	1425	1450	1500	1525
SiO_2	47.47	48.74	47.97	48.37	45.67	46.77
TiO_2	0.75	0.51	0.83	0.69	0.99	0.55
Al_2O_3	15.53	13.16	14.88	13.80	14.33	12.87
FeO*	8.51	8.80	9.43	8.47	9.59	9.81
MnO	0.18	0.24	0.00	0.07	0.17	0.29
MgO	13.94	15.69	13.36	15.88	16.73	17.82
CaO	11.11	11.06	10.23	10.93	10.64	10.63
Na_2O	2.22	1.37	2.37	1.46	1.80	0.87
K_2O	0.08	0.13	0.82	0.15	0.07	0.09
Cr_2O_3	0.21	0.30	0.11	0.18	0.21	0.30
Total	100.00	100.00	100.00	100.00	100.00	100.00
CIPW norm						
os	0.47	0.77	4.85	0.89	0.42	0.53
ab	17.14	11.62	15.87	12.38	11.18	7.38
an	32.25	29.46	27.57	30.72	30.85	31.05
ne	0.89		2.28		2.22	
di	18.49	20.57	18.77	18.91	17.72	17.58
hy		14.64		11.85		13.17
ol	29.33	21.97	29.09	23.94	35.72	29.25
il	1.42	0.97	1.58	1.31	1.89	1.05
Fo (mol%)	90.2	90.8	90.5	91.2	90.1	90.8
K_d (Fe/Mg)	0.317	0.322	0.265	0.323	0.341	0.328
F [a]	0.135	0.219	0.126	0.206	0.166	0.347

Decay scheme of natural ^{238}U, and spontaneous and induced fission of ^{238}U and ^{235}U

Nuklid	Zerfall	HWZ	E / MeV	Zerfallsprodukt
^{238}U	α	$4{,}468 \cdot 10^9$ a	4,270	^{234}Th
^{234}Th	β^-	24,10 d	0,198	^{234m}Pa
^{234m}Pa	β^- 99,84 % IT 0,16 %	1,17 min	2,271 0,074	^{234}U ^{234}Pa
^{234}Pa	β^-	6,7 h	2,197	^{234}U
^{234}U	α	245500 a	4,859	^{230}Th
^{230}Th	α	75380 a	4,770	^{226}Ra
^{226}Ra	α	1602 a	4,871	^{222}Rn
^{222}Rn	α	3,8235 d	5,590	^{218}Po
^{218}Po	α 99,98 % β^- 0,02 %	3,05 min	6,115 0,265	^{214}Pb ^{218}At
^{218}At	α 99,90 % β^- 0,10 %	1,5 s	6,874 2,883	^{214}Bi ^{218}Rn
^{218}Rn	α	35 ms	7,263	^{214}Po
^{214}Pb	β^-	26,8 min	1,024	^{214}Bi
^{214}Bi	β^- 99,98 % α 0,02 %	19,9 min	3,272 5,617	^{214}Po ^{210}Tl
^{214}Po	α	164 µs	7,883	^{210}Pb
^{210}Tl	β^- 99,9930 % β^-n 0,0070 %	1,30 min	5,484 0,299	^{210}Pb ^{209}Pb
^{210}Pb	β^- ≈ 100 % α $1{,}9 \cdot 10^{-6}$ %	22,3 a	0,064 3,792	^{210}Bi ^{206}Hg
^{210}Bi	β^- 99,99987 % α 0,00013 %	5,013 d	1,161 5,036	^{210}Po ^{206}Tl
^{206}Hg	β^-	8,15 min	1,308	^{206}Tl
^{210}Po	α	138,376 d	5,407	^{206}Pb
^{206}Tl	β^-	4,199 min	1,533	^{206}Pb
^{206}Pb	-	stabil	-	-

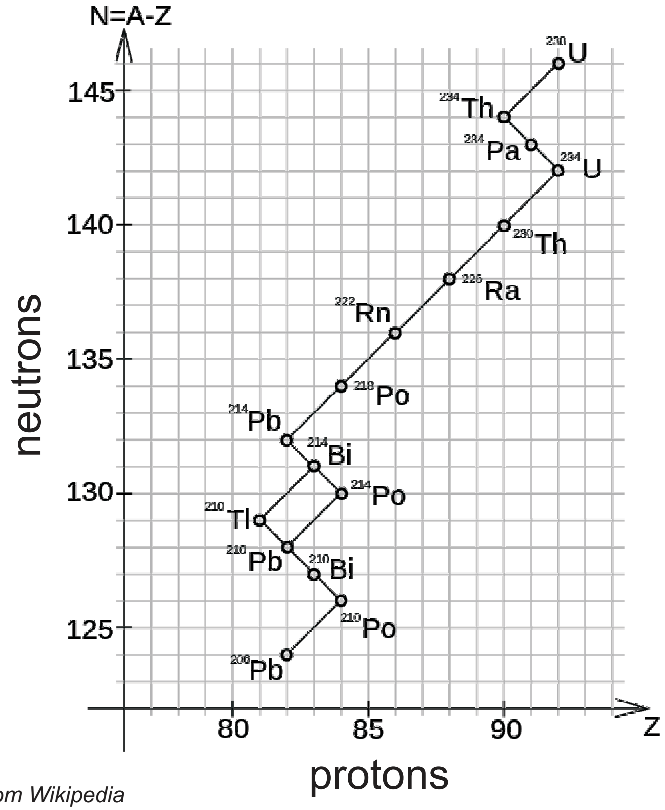

From Wikipedia

$A_1 = A_2 = \ldots = A_n$

$A_{238} = A_{234} = \ldots = A_{206}$

$A(t) = \lambda \times N(t)$

$T_{1/2} = \ln(2)/\lambda$

A = Activity (decays/time)
Unit: Bequerel (Bq)
1 Bq = 1 decay/sec
1 Curie (Ci) = 3.7×10^{10} Bq

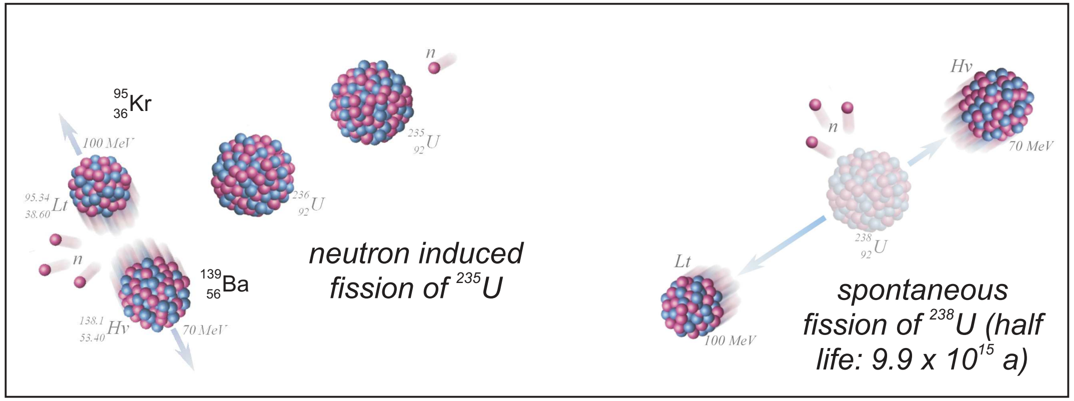

neutron induced fission of ^{235}U

spontaneous fission of ^{238}U (half life: 9.9×10^{15} a)

Composition of the Continental Crust (Rudnick & Gao, 2003, Treatise on Geochemistry)

Table 11 Comparison of the upper, middle, lower and total continental crust compositions recommended here.

Element	*Upper crust*	*Middle crust*	*Lower crust*	*Total crust*
SiO_2	66.6	63.5	53.4	60.6
TiO_2	0.64	0.69	0.82	0.72
Al_2O_3	15.4	15.0	16.9	15.9
FeO_T	5.04	6.02	8.57	6.71
MnO	0.10	0.10	0.10	0.10
MgO	2.48	3.59	7.24	4.66
CaO	3.59	5.25	9.59	6.41
Na_2O	3.27	3.39	2.65	3.07
K_2O	2.80	2.30	0.61	1.81
P_2O_5	0.15	0.15	0.10	0.13
Total	100.05	100.00	100.00	100.12
Mg#	46.7	51.5	60.1	55.3
Li	24	12	13	16
Be	2.1	2.3	1.4	1.9
B	17	17	2	11
N	83		34	56
F	557	524	570	553
S	621	249	345	404
Cl	294	182	250	244
Sc	14.0	19	31	21.9
V	97	107	196	138
Cr	92	76	215	135
Co	17.3	22	38	26.6
Ni	47	33.5	88	59
Cu	28	26	26	27
Zn	67	69.5	78	72
Ga	17.5	17.5	13	16
Ge	1.4	1.1	1.3	1.3
As	4.8	3.1	0.2	2.5
Se	0.09	0.064	0.2	0.13
Br	1.6		0.3	0.88
Rb	82	65	11	49
Sr	320	282	348	320
Y	21	20	16	19
Zr	193	149	68	132
Nb	12	10	5	8
Mo	1.1	0.60	0.6	0.8
Ru	0.34		0.75	0.57
Pd	0.52	0.76	2.8	1.5
Ag	53	48	65	56
Cd	0.09	0.061	0.10	0.08
In	0.056		0.05	0.052
Sn	2.1	1.30	1.7	1.7
Sb	0.4	0.28	0.10	0.2
I	1.4		0.14	0.71
Cs	4.9	2.2	0.3	2
Ba	628	532	259	456
La	31	24	8	20
Ce	63	53	20	43
Pr	7.1	5.8	2.4	4.9
Nd	27	25	11	20
Sm	4.7	4.6	2.8	3.9
Eu	1.0	1.4	1.1	1.1
Gd	4.0	4.0	3.1	3.7
Tb	0.7	0.7	0.48	0.6
Dy	3.9	3.8	3.1	3.6
Ho	0.83	0.82	0.68	0.77
Er	2.3	2.3	1.9	2.1

(continued)

Table 11 (continued).

Element	*Upper crust*	*Middle crust*	*Lower crust*	*Total crust*
Tm	0.30	0.32	0.24	0.28
Yb	2.0	2.2	1.5	1.9
Lu	0.31	0.4	0.25	0.30
Hf	5.3	4.4	1.9	3.7
Ta	0.9	0.6	0.6	0.7
W	1.9	0.60	0.60	1
Re	0.198		0.18	0.188
Os	0.031		0.05	0.041
Ir	0.022		0.05	0.037
Pt	0.5	0.85	2.7	1.5
Au	1.5	0.66	1.6	1.3
Hg	0.05	0.0079	0.014	0.03
Tl	0.9	0.27	0.32	0.5
Pb	17	15.2	4	11
Bi	0.16	0.17	0.2	0.18
Th	10.5	6.5	1.2	5.6
U	2.7	1.3	0.2	1.3
Eu/Eu*	0.72	0.96	1.14	0.93
Heat production ($\mu W\ m^{-3}$)	1.65	1.00	0.19	0.89
Nb/Ta	13.4	16.5	8.3	12.4
Zr/Hf	36.7	33.9	35.8	35.5
Th/U	3.8	4.9	6.0	4.3
K/U	9475	15607	27245	12367
La/Yb	15.4	10.7	5.3	10.6
Rb/Cs	20	30	37	24
K/Rb	283	296	462	304
La/Ta	36	42	13	29

Cerny, 1991

Table 1 Composition of typical fertile granites.

	1 – Osis Lake			2 – Lac du Bonnet	
	biotite granite	coarse-grained leucogranite	pegmatitic leucogranite	leucogranite	pegmatitic leucogranite
SiO_2 (wt%)	73.15	75.40	72.72	76.56	75.75
TiO_2	0.12	0.06	0.04	0.10	0.03
Al_2O_3	14.40	14.33	15.36	12.36	14.07
Fe_2O_3	0.46	0.72	0.61	1.07	0.36
FeO	1.05	0.28	0.68	0.56	0.15
MnO	0.03	0.08	0.06	0.03	0.01
MgO	0.48	0.13	0.06	0.10	0.09
CaO	0.76	0.72	0.29	0.56	0.68
Na_2O	3.12	4.09	4.44	3.65	4.20
K_2O	5.42	2.83	4.78	4.65	5.24
P_2O_5	0.15	0.16	0.49	0.02	0.00
CO_2	0.03	0.08	0.11	0.05	0.03
H_2O^+	0.88	0.67	0.46	0.36	0.22
F_2	0.02	0.04	0.02	0.01	0.02
$-O=F_2$	0.01	0.02	0.01	–	0.01
total	100.07	99.57	100.11	100.08	100.85
A/CNK **	1.16	1.29	1.18	1.02	1.12
A/NK **	1.31	1.46	1.23	1.02	1.12
Li (ppm)	71	63	10	28	–
Rb	187	137	343	216	244
Cs	15.4	8.4	8.4	2.9	–
Be	0.7	0.8	0.8	2.9	–
Sr	83	26	44	30	33
Ba	287	8	14	398	103
Ga	28	48	43	32	47
Y	nd	28	nd	51	19
U	30	23	3.5	9.9	2
Th	nd	6.7	nd	39	8
Zr	78	38	13	196	9
Hf	1.63	3.05	0.34	7.4	1.8
Sn	4.8	13	20	7.9	5
K/Rb	237	132	117	194	178
K/Ba	162	5402	7010	492	422
Ba/Rb	1.53	0.06	0.04	2.2	0.42
Rb/Sr	2.25	5.3	7.8	9.5	7.6
Mg/Li	39.7	11.5	31	25.6	–
Zr/Sn	16.3	2.9	0.7	22	2.1
Zr/Hf	47.8	12.4	5.8	27.5	12.8
Al/Ga	2737	1674	1890	2087	1586
Th/U	0.1	0.3	0.1	2.75	2.75

Notes

1 Peraluminous LCT granite grading from biotite through two-mica + garnet to muscovite + garnet + tourmaline types (from Černý and Brisbin, 1982)

2 Metaluminous NYF fertile granite with biotite and extremely rare garnet (from Černý *et al.*, 1987)

–, not determined; nd, not detected

** A = molecular Al_2O_3, CNK = $CaO + Na_2O + K_2O$, and NK = $Na_2O + K_2O$